International Journal of Multiphase Flow 79 (2016) 172–180

Contents lists available at ScienceDirect

International Journal of Multiphase Flow

journal homepage: www.elsevier.com/locate/ijmultiphaseflow

Development of self-aeration process for supercritical chute flows

Wangru Wei, Jun Deng*, Faxing Zhang

State Key Laboratory of Hydraulics and Mountain River Engineering, Sichuan University, 610065 Chengdu, China

ARTICLE INFO

Article history:
Received 12 December 2014
Revised 6 November 2015
Accepted 15 November 2015

Keywords:
Self-aeration
Air concentration
Developing region
Chute flow
Hydraulic model experiment

ABSTRACT

When a high-velocity flow discharges into a chute, air is entrained through the free surface. This is relevant to the development of self-aeration for mixture flow. In this study, the air concentration was measured in the self-aerated developing region for various initial flow velocities, depths, and chute slopes. The effect of hydraulic conditions on the bottom self-aeration process was analyzed. Increasing the initial flow velocity and depth was found to increase the rate of air diffusion into the water flow. This positive correlation indicates that flow turbulence is a key factor for the self-aeration development process. The Reynolds number of the flow was found to be an appropriate hydraulic condition for describing self-aeration development. In addition, the constraint of buoyancy on air bubble diffusion into the chute bottom decreased as the chute slope was increased, which made the development process for bottom self-aeration more pronounced. A new empirical equation is presented for predicting the development process of bottom self-aeration in open channel flows.

Introduction

When high-velocity water flows down a chute, the free surface aeration generates (Fig. 1). As the air entrainment develops, bubbles penetrate the water towards the chute bottom along the flow direction until a two-phase flow fully develops and becomes uniform, where the turbulence intensity counterbalances the buoyancy effect exactly and the air concentration is independent of the flow direction.

A large amount of data on the fully developed uniform region is available for predicting the air-water flow properties of supercritical chute flows (Straub and Anderson, 1958; Wood, 1991; Deng et al., 2002 and 2003). Wood (1983) and Hager (1991) investigated the relationship between the air concentration and hydraulic conditions including the flow discharge and channel slope in uniform flows. Basic equations for the uniform aerated region were developed based on turbulent diffusion theory (Chanson 1993). However, there is little literature on the self-aerated developing region in chute flows, especially the bottom self-aeration process along the flow downstream, and the relationship between the flow conditions and slope. Chanson (1997a, 1997b) studied the aerated developing region in a flat chute and described the flow structure, but only one chute slope (4°) was tested, and the maximum mean air content of the cross-section was only 0.12.

The Froude number has been used as the hydraulic condition in many previous investigations on air transport in air–water flows (Pfister and Hager, 2010a and 2010b; Pagliara et al., 2011). Kramer and Hager (2005) investigated air bubble transportation in air–water flows over a chute aerator. Pfister and Hager (2011) studied the development process of self-aeration in a stepped spillway flow from the spillway crest. These studies suggested the air–water structure to be a function of the Froude number of the flow. This is because the cavity characteristics (hollow niches for stepped spillways and rough-rock chutes) were the main considerations in these aeration situations (Guenther et al., 2013; Felder and Chanson, 2014), and the jet length, which is affected by the Froude number, is often used as a characteristic parameter to compute the air entrainment capacity. However, the applicability of the Froude number to the free surface self-aeration conditions of high turbulent chute flows is still unclear, especially the validity of the relationship between the results of a physical model and prototype situations. This is related to "the notion of scale effects which is closely linked with the section of some characteristics turbulent flow properties" (Chanson 2013).

This work aimed to provide some understanding of the self-aeration development process in supercritical chute flows. Various conditions of the approach flow velocity, depth, and chute slope were examined. The total conveyed air (i.e., sum of entrapped and entrained air as proposed by Wilhelms and Gulliver (2005)) was measured, and the effects of the flow conditions and chute slope were analyzed. An explicit relationship was presented for predicting the bottom self-aeration process.

* Corresponding author. Tel.: +86 159 0285 4895.
E-mail addresses: wangru_wei@hotmail.com (W. Wei), djhao2002@scu.edu.cn (J. Deng).

http://dx.doi.org/10.1016/j.ijmultiphaseflow.2015.11.003
0301-9322/

Fig. 1. Free-surface aeration: (a) spillway in Huangtan Dam (Hu et al. 2012); (b) steep chute in Wudu Dam (Imaged by Jun Deng).

Hydraulic model

Experiments were performed in two model chutes fabricated from polymethyl methacrylate (PMMA). One chute was 12 m long and 0.4 m wide with a bottom angle of $\alpha = 7.5°–17.5°$ (Fig. 2a). The other was 18 m long and 0.3 m wide with $\alpha = 28°$ (Fig. 2b). Here, x = stream-wise coordinate along the chute bottom, and y = coordinate in the perpendicular direction. The roughness height of the model chutes was 0.01 mm. Hsiao (1947) and Wilhelms (1997) showed that the air concentration at the center of the channel is homogeneous in the transverse direction of a 6-in-wide (15.24 cm-wide) channel. This suggests that the effects from a smooth sidewall may be neglected and that the assumption of transverse homogeneity should likewise be valid for the chutes of the present study.

The flow to the chute was fed through a smooth convergent nozzle, and the initial water depth d_0 was variable. The central stream-wise air concentration distribution was measured with a phase-detection needle probe (CQY-Z8a Measurement Instrument, China; Chen and Shao 2006). The measurement was based on using the different voltage indices at the platinum tip between the air and water phases. The profiles were measured at the flow cross-sections perpendicular to the chute bottom at intervals of 2–3 mm up to the free surface. At different scanning times (t = 2–40 s) and sampling frequencies (F_{sample} = 20–300 kHz), the air concentration and air bubble frequency were almost stable at a certain measured point, as shown in Fig. 3. Thus, the scanning time and sampling frequency were considered to have no effects on the experimental results in the present study. The signals from the conductivity probe were recorded at a scan rate of F_{sample} = 200 kHz per channel for a scan period of t = 5 s.

Approach flows with variable initial depths d_0, velocities V_0, relative Reynolds number $Re_0 = V_0 D_0/\nu$, and Froude numbers $Fr_0 = V_0/(gd_0)^{0.5}$ were generated in the intake connected to the chute, where ν = kinematic water viscosity and g = gravitational acceleration. D_0 is the hydraulic diameter of the initial water flow in the chute and is defined as

$$D_0 = \frac{W d_0}{W + 2d_0}, \tag{1}$$

where W is the chute width. The initial average water velocity V_0 is defined as

$$V_0 = \frac{q_w}{d_0}, \tag{2}$$

where q_w is the unit flow discharge. Four series tests were conducted, as presented in Table 1, including different hydraulic conditions.

Air concentration characteristics

Detailed air concentration profiles at different flow cross-sections along the stream-wise were measured for all the tests (Table 1), and the documentation are available as digital supplementary data (see Electronic Annex 1 in the online version of this article). Fig. 4 shows typical air concentration profiles at flow cross-sections. The previous studies of Wood (1983) and Chanson (1995) used the characterized aerated flow depth y_{90} (where the air concentration was 0.90) as the dimensionless method for the fully developed uniform zone of a self-aerated flow. For the developing zone, the variation in y_{90} is related to the initial test conditions, including the approach V_0, d_0, and α. Thus, the parameter y/d_0 describes the dimensionless air concentration distribution at the cross-section considering the initial water depth d_0 as a variable in this study.

Based on the Chézy theory for an open-channel flow, a uniform water flow corresponds to a specific flow condition for a certain slope in principle; this includes the flow velocity and hydraulic radius. In the present study, the initial velocities in all tests with different approach flow depths and chute slopes were generally less than the theoretical value for a uniform condition, as shown in Fig. 5. For a small chute slope ($\alpha = 9.5°\sim13.5°$) and initial flow hydraulic radius D_0 = 0.038 m, the difference between the test and theoretical velocities was relatively small, and the variation in the air-water flow depth along the stream-wise direction was not significant considering the enhancement effect of self-aeration on the flow depth (Fig. 4(a)). For a large chute slope ($\alpha = 28°$) and initial flow depth D_0 = 0.052–0.067 m, the variation in the air–water flow depth along the stream-wise direction was more pronounced and was caused by the greater difference between the actual and theoretical velocities (Fig. 4(b)). Thus, the present tests mainly considered the non-uniform accelerating process.

The mean cross-sectional air concentration C_{mean} is defined as the integration of the local values $C(y)$ over the flow depth between the chute bottom at $y = 0$ and the free surface y_{90}:

$$C_{mean} = \frac{1}{y_{90}} \int_{y=0}^{y_{90}} C(y) dy \tag{3}$$

Fig. 6 shows the stream-wise variation of the mean cross-sectional air concentration (S1-1–S1-5). For all test series (Electronic Annex 1), C_{mean} increased in the stream-wise direction downstream. According to Hager (1991), the average air concentration C_{mean} for a uniform air–water mixture flow in an open channel is given by

$$C_{mean} = 0.75(\sin\alpha)^{0.75}. \tag{4}$$

For the present slope conditions of $\alpha = 9.5°$, 13.5°, 17.5°, and 28°, the mean air concentrations for a uniform aerated flow should be 0.19, 0.25, 0.30, and 0.43, respectively. The measured amount of air entrainment was relatively low. Thus, the self-aeration in the test area was in the developing zone, and the mixed air-water flow did not reach the fully developed uniform region.

For all tests, the average air concentration was already greater than 0.03–0.05 at about $x/d_0 = 5$. This indicates that self-aeration

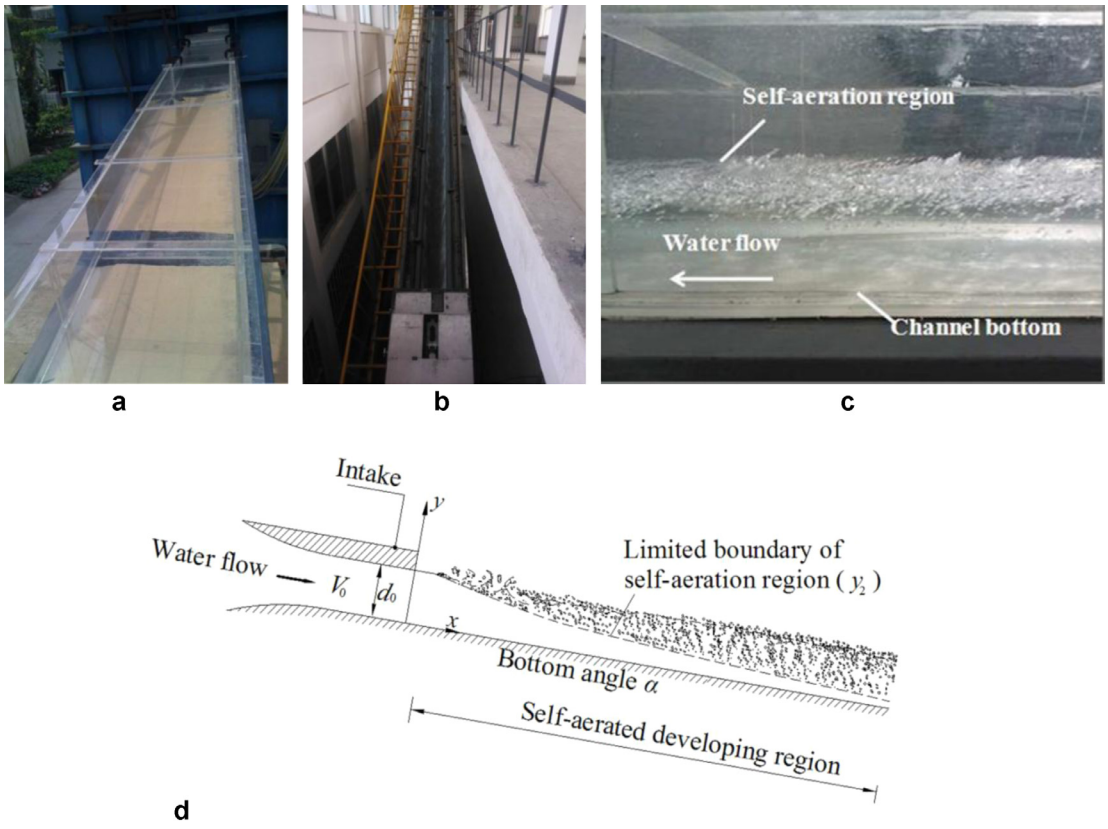

Fig. 2. Chute model: (a) 40 cm wide, (b) 30 cm wide; self-aerated air-water flow: (c) typical photography, (d) definition sketch.

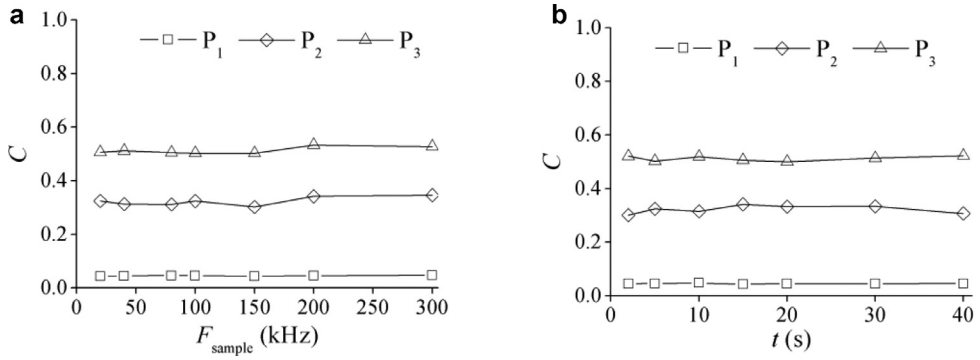

Fig. 3. Effects of sampling frequency (a) and scanning time (b) on the measurement ($V_0 = 6.4$ m/s, $d_0 = 0.05$ m, $P_1: x/d_0 = 86, y/d_0 = 0.90$; $P_2: x/d_0 = 24, y/d_0 = 1.02$; $P_3: x/d_0 = 116, y/d_0 = 0.70$).

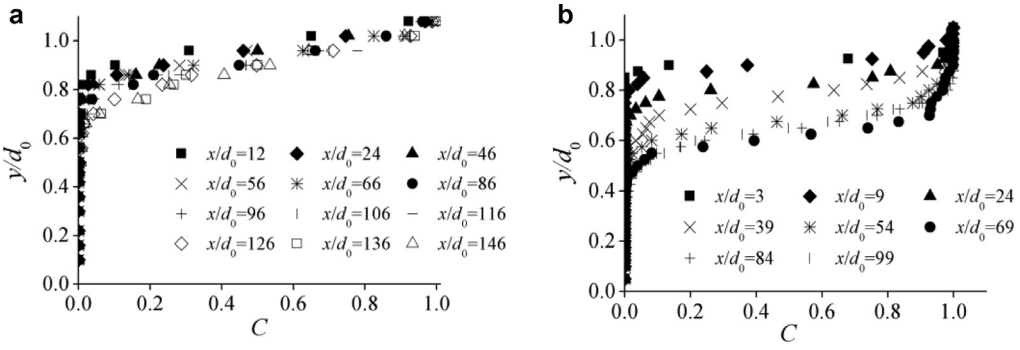

Fig. 4. Air concentration profiles at flow cross-section: (a) S1-5; (b) S4-9.

Table 1
Test program and turbulence parameter.

Series	Test number	α (°)	W (m)	d_0 (m)	V_0 (m/s)	q_w (m^2/s)	Re_0 ($\times 10^5$)	Fr_0
S1	1	9.5	0.4	0.05	3.5	0.175	1.1	5.0
	2			0.05	4.5	0.225	1.4	6.4
	3			0.05	5.5	0.275	1.7	7.9
	4			0.05	6.0	0.300	1.8	8.6
	5			0.05	6.5	0.325	2.0	9.3
	6			0.08	4.5	0.360	2.0	5.1
	7			0.08	5.2	0.416	2.3	5.9
	8			0.08	6.1	0.488	2.7	6.9
	9			0.08	6.6	0.528	2.9	7.5
S2	1	13.5	0.4	0.05	3.5	0.175	1.1	5.0
	2			0.05	4.3	0.215	1.3	6.1
	3			0.05	5.0	0.250	1.5	7.1
	4			0.05	5.8	0.290	1.8	8.3
	5			0.05	6.4	0.320	2.0	9.1
S3	1	17.5	0.4	0.05	4.5	0.225	1.4	6.4
	2			0.05	5.2	0.260	1.6	7.4
	3			0.05	6.0	0.300	1.8	8.6
	4			0.05	7.0	0.350	2.1	10.0
	5			0.05	7.8	0.390	2.4	11.1
S4	1	28	0.3	0.05	6.2	0.310	1.8	8.9
	2			0.05	7.5	0.375	2.1	10.7
	3			0.05	9.0	0.450	2.6	12.9
	4			0.08	6.6	0.528	2.6	7.5
	5			0.08	7.5	0.600	3.0	8.5
	6			0.08	8.5	0.680	3.4	9.6
	7			0.10	6.5	0.650	3.0	6.6
	8			0.10	7.5	0.750	3.4	7.6
	9			0.10	8.4	0.840	3.8	8.5
	10			0.12	6.2	0.744	3.2	5.7
	11			0.12	7.0	0.840	3.6	6.5

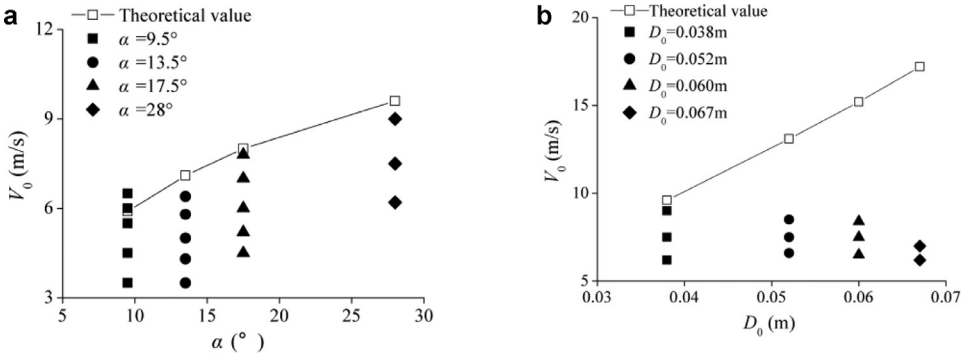

Fig. 5. Comparison of test and theoretical uniform flow velocities: (a) chute slope variation; (b) hydraulic radius variation.

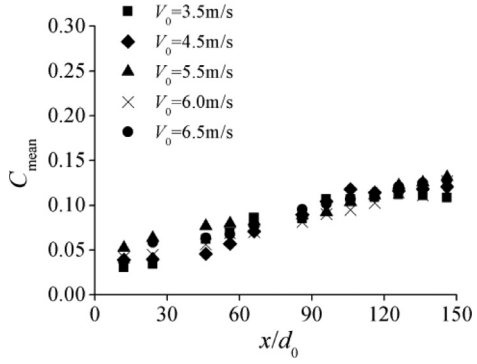

Fig. 6. Stream-wise variations of mean cross-sectional air concentration (α = 9.5°, d_0 = 0.05 m).

occurs closer to the chute intake. For a high-velocity flow discharging into a flat chute, the inception point of self-aeration located much more upstream compared to a situation where a steady free surface flows over a crest weir (Arreguin and Echavez, 1986; Anwar, 1994). Thus, the interaction between flow surface and gate lip cannot be excluded.

Effects of flow conditions on limited boundary of self-aeration

Effect of initial flow velocity

With development of bottom self-aeration process develops downstream, the characteristic position representing the limited bottom boundary of entrained air penetration into the water flow is defined as y_2, where the air concentration $C = 0.02$. This is derived from the measured air concentration. This definition is relevant to cavitation protection based on the previous literature, including experimental tests and prototype measurements (Rasmussen, 1956; Russell and Sheehan, 1974). The coefficient y_2/d_0 describes the bottom self-aeration process in the air–water flow. Fig. 7 shows typical bottom self-aeration profiles along the stream-wise direction (S1-1–S1-5). As the approach flow velocity increases, the bottom self-aeration profile becomes closer to the chute bottom (Electronic Annex 1). This means

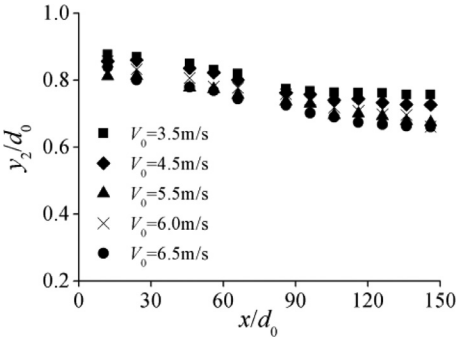

Fig. 7. Effects of V_0 on stream-wise development of y_2/d_0 for test series ($\alpha = 9.5°$, $d_0 = 0.05$ m).

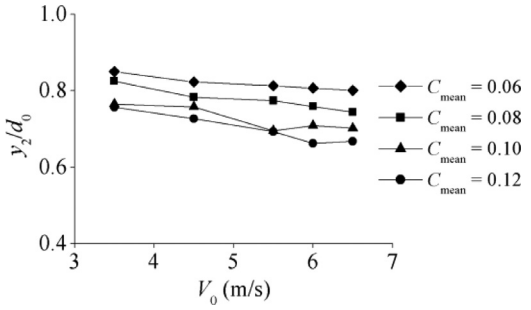

Fig. 8. Effect of V_0 on y_2/d_0 for identical aeration conditions ($d_0 = 0.05$ m, $\alpha = 9.5°$).

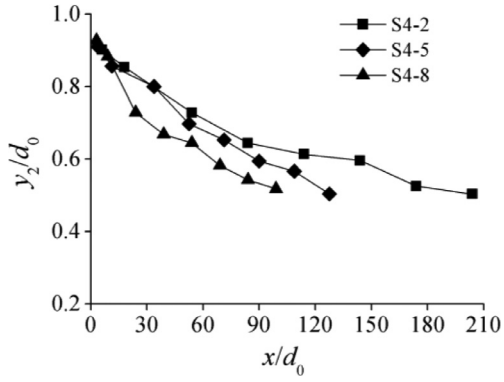

Fig. 9. Effects of d_0 on stream-wise development of y_2/d_0 ($V_0 = 7.5$ m/s, $\alpha = 28°$).

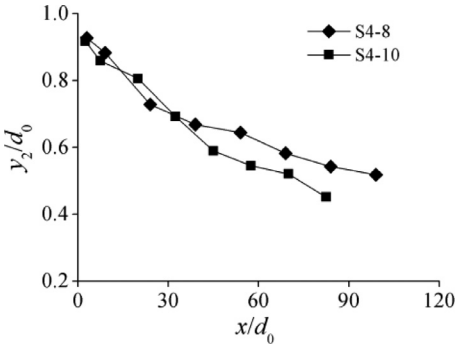

Fig. 10. Effects of q_w on stream-wise development of y_2/d_0 ($q_w = 0.750$ m^2/s).

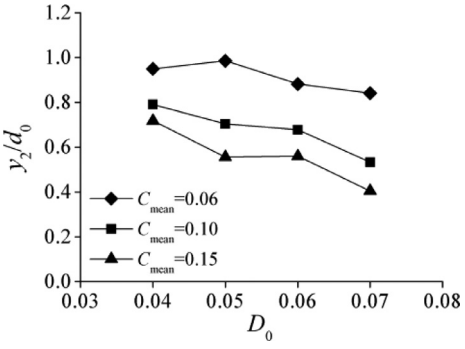

Fig. 11. Effects of D_0 on stream-wise development of y_2/d_0 ($V_0 = 6.5$ m/s, $\alpha = 28°$).

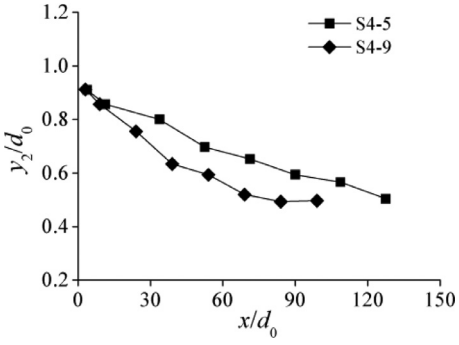

Fig. 12. Stream-wise development of y_2/d_0 for identical Fr_0 ($\alpha = 28°$, $Fr_0 = 8.5$).

that the aeration becomes more intensive, and the bubble diffusion becomes more rapid. Bubble diffusion into the flow is more pronounced in the upper region of $0 < x/d_0 < 60$~80. For $x/d_0 > 60$~80, the variation of diffusion tendency gets much gently. This indicates that the self-aeration intensity gradually decreases as air entrainment developing uniform.

As shown in Fig. 8, the y_2/d_0 profiles were located closer to the chute bottom for the same flow aeration (identical C_{mean}) and increasing V_0. This trend was more pronounced for larger C_{mean}. The development of self-aeration was mainly improved because the higher velocity increases the water flow turbulence, which strengthens the diffusion of single bubbles and air-water clusters into the flow while overcoming the buoyancy effect. According to previous studies (Wang et al. 1990), the presence of bubbles in self-aerated flows should increase the turbulence level, which contributes to the bottom self-aeration process for greater C_{mean} values.

Effect of initial flow depth

Fig. 9 shows the bottom self-aeration profiles for different initial water depths with generally identical V_0 and α condition. For larger d_0, the bottom self-aeration profiles were located closer to chute bottom. As approach flow depth increased, the development of bottom self-aeration process became more rapid. This trend holds for almost whole process of self-aeration development ($0 < x/d_0 < 150$–240, Electronic Annex 1).

The approach flow depth changes three flow conditions: the flow discharge q_w, flow pattern Fr_0, and turbulence Re_0. Fig. 10 shows the bottom self-aeration processes for the same q_w. The corresponding trend curves are not coincident, which indicates that the reason is not the difference in flow discharge. For open channel flows, the hydraulic diameter is a parameter that represents the flow turbulence level. As increases d_0, D_0 increases for a constant chute wide. The flow turbulence level increases with this variation in the wall boundary condition. This effect enhances the bubble diffusion into the water flow, as shown in Fig. 11. For the same flow aeration (identical C_{mean}), the bottom self-aeration locates closer to the chute

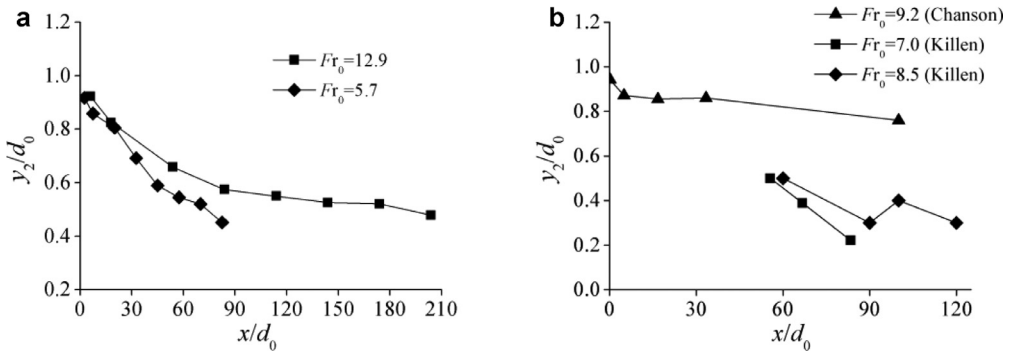

Fig. 13. Effect of Fr_0 on stream-wise y_2/d_0: (a) present study; (b) previous studies.

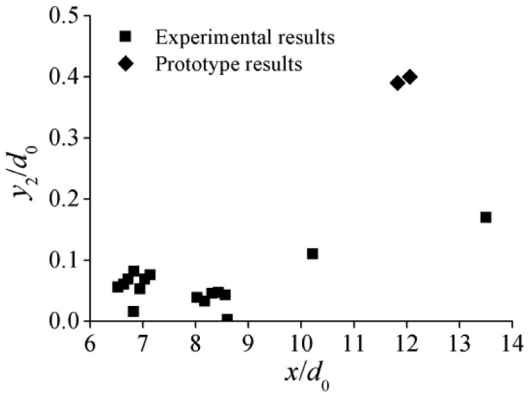

Fig. 14. Effect of Fr_0 on u_r in self-aerated chute flows.

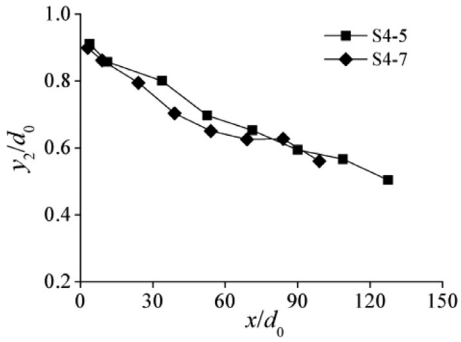

Fig. 15. Stream-wise development of y_2/d_0 self-aeration for identical Re_0 ($\alpha = 28°$, $Re_0 = 3.0\times10^5$).

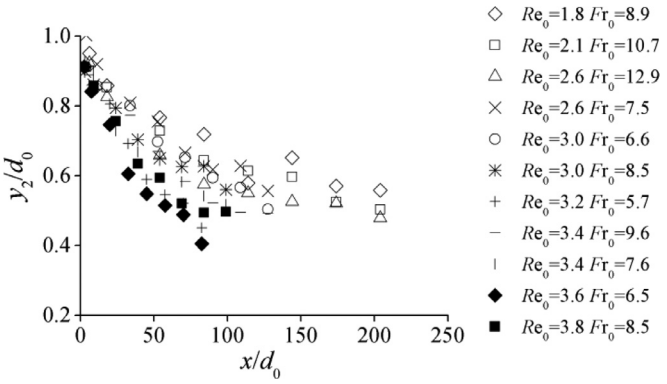

Fig. 16. Effects of Re_0 and Fr_0 on stream-wise development of y_2/d_0 (The Re_0 is $\times10^5$).

bottom with increase of D_0. The effect of d_0 on Froude number and Reynolds number is discussed in the following section.

Effects of Fr_0 and Re_0 on bottom self-aeration process

Fig. 12 gives the bottom self-aeration profiles for identical initial flow Froude number and chute slope conditions. For the two same approach flow Fr_0, the bottom self-aeration profiles are not coincident. This is mainly because V_0 and d_0 are both positive-correlated with air bubble diffusion into the flow, as shown in the above test results. Fig. 13 shows the bottom self-aeration profiles for different Fr_0, considering the previous studies (Killen, 1968; Chanson, 1997a). With the increase of Fr_0, the bubble diffusion gets weakened. Both of the above results show that the Froude number of the flow may mislead to the prediction of self-aeration development in chute flows.

In a self-aerated flow, the air bubble rise velocity u_r is a key factor for the diffusion process. Fig. 14 summarizes a series of bubble velocity u_r values for different Fr_0 in self-aerated flows. The values of u_r in the model and prototype self-aerated flows (Straub and Lamb, 1956; Isachenko, 1965; Xi, 1988) were determined from the theory proposed by Chanson (1993). When $Fr_0 < 10$, small and large values of Fr_0 generate almost the same u_r, while it becomes slightly larger but oscillates greatly when $Fr_0 > 10$. This shows that the Froude number cannot be used to accurately estimate the air bubble movement in a self-aerated flow.

Fig. 15 gives the bottom self-aeration profiles for identical initial flow Reynolds number and chute slope conditions. For the two same Re_0 approach flow situations, the two profiles are essentially coincident. Fig. 16 shows the effects of Re_0 and Fr_0 on the bottom self-aeration process for all test series. For greater Re_0, the bottom self-aeration profiles become closer to the chute bottom, and the air bubble diffusion capacity is greater than that for smaller Re_0. However, no clear trend for the effect of the Froude number was observed. Considering that flow Reynolds number affects the turbulence intensity, a higher Re_0 represents a greater inertial force (at y-direction) exerted by the air bubble to overcome buoyancy in the flow. Thus, it makes a positive contribution to the air bubble turbulent transport capacity. Therefore, the Reynolds number of the flow should be considered as an appropriate hydraulic parameter for describing the development of self-aeration in chute flows.

Effect of chute slope on bottom self-aeration process

Fig. 17 shows the isolated effect of the chute slope α ($9.5° \le \alpha \le 28°$) on the bottom self-aeration process. For $1.1 \times 10^5 \le Re_0 \le 1.8 \times 10^5$, the extended curves of the y_2/d_0 profiles did not show a significant difference. For $2.0 \times 10^5 \le Re_0 \le 3.0 \times 10^5$, the bottom self-aeration process improved with α. The effect of α variation on the bottom self-aeration process is not pronounced for low flow turbulence. However, increasing the flow turbulence level makes

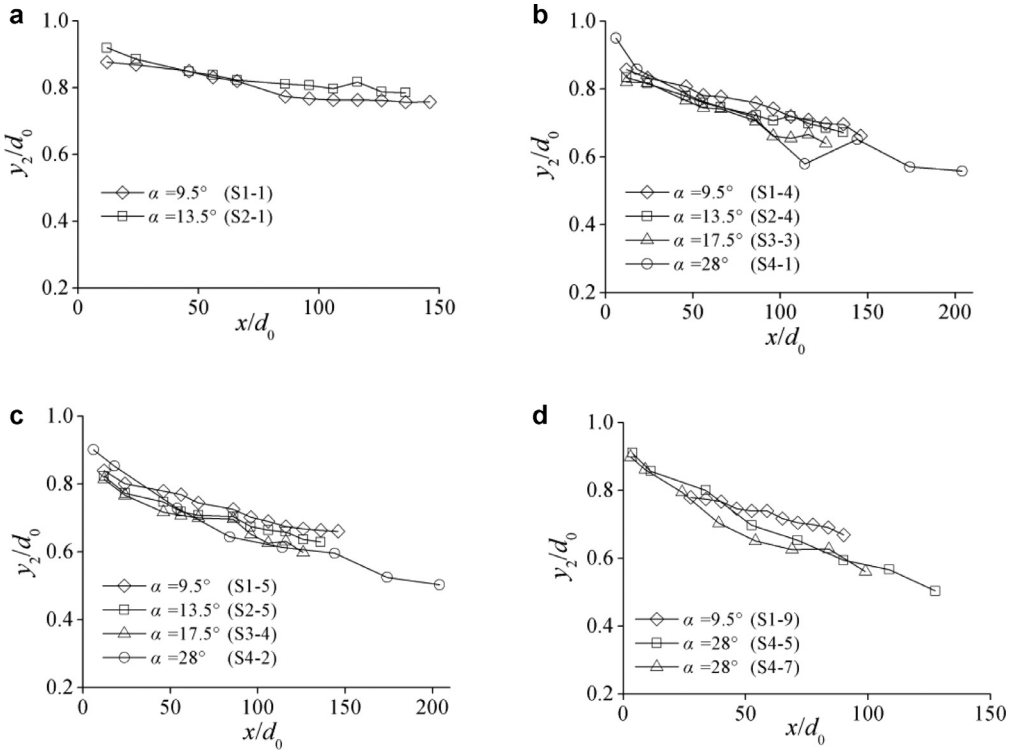

Fig. 17. Effect of chute slope α on stream-wise y_2/d_0: (a) $Re_0 = 1.1\times10^5$; (b) $Re_0 = 1.8\times10^5$; (c) $Re_0 = 2.0\times10^5$; (d) $Re_0 = 3.0\times10^5$.

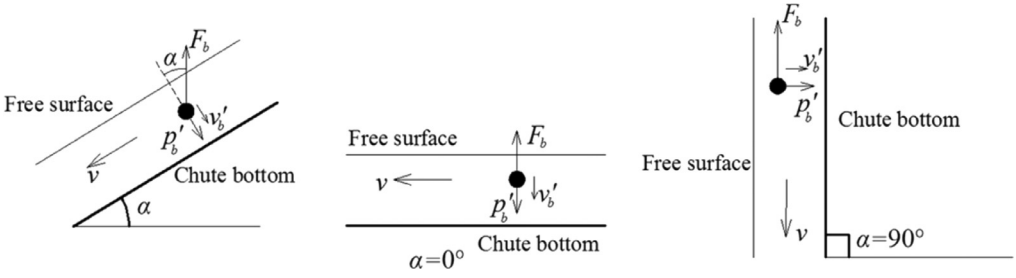

Fig. 18. Dynamic process of entrained bubble transportation in air-water flows.

the difference more pronounced in the bottom self-aeration process caused by the chute slope.

Entrained air bubbles in the self-aerated flow are transported by flow turbulence with overcoming buoyancy effect. The turbulent force p_b' on bubble is characterized by the turbulent velocity v_b' at direction normal to the chute bottom, as shown in Fig. 18. The buoyancy force F_b on the bubble is in the direction opposite to gravity. The resulting force F_R between turbulence and buoyancy, with viscosity neglected, becomes,

$$F_R = p' - F_b \cdot \cos\alpha \tag{5}$$

Considering the turbulence and buoyancy are constant, the buoyancy has a strong suppression effect for $\alpha = 0°$ (i.e., the chute is horizontal), and it is the most difficult situation for bubble diffusion. For $\alpha = 90°$ (i.e., the chute flow is a wall jet), the bubble transport process at y direction is independent of the buoyancy effect, and the flow turbulence prompts bottom self-aeration process most prominently. Because all of the present tests were performed under flat chute conditions with $9.5° \le \alpha \le 28°$, the constraining effect of buoyancy was the main factor. As the flow turbulence level was increased, the difference caused by slope variation gradually became more pronounced.

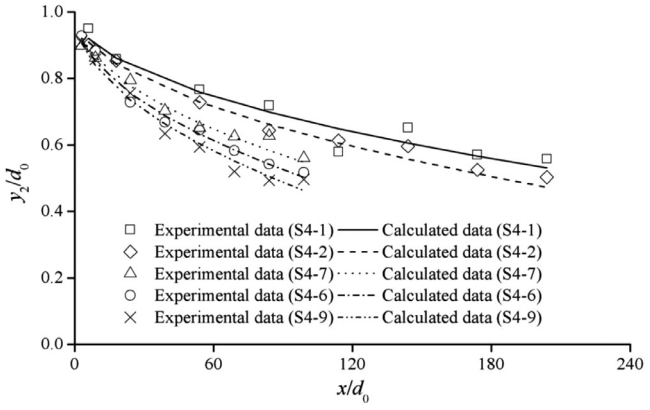

Fig. 19. Comparison of bottom self-aeration process between experimental data and Eq. (6) ($\alpha = 28°$).

Prediction of bottom self-aeration process

The bottom self-aeration process represents a basic factor to specify the general air bubble transportation in self-aerated flows.

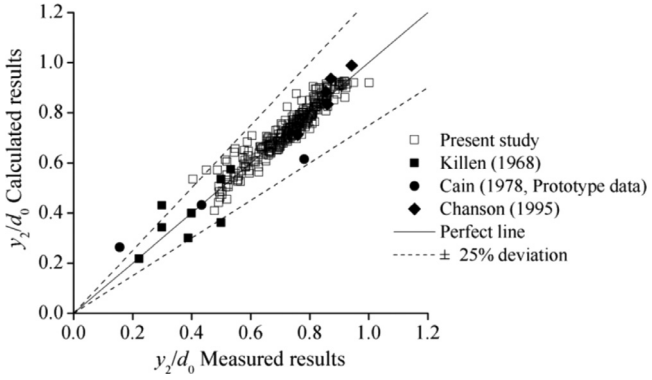

Fig. 20. Comparison of test data with Eq. (6).

Considering the effects of flow turbulence and chute slope situations, the following relationship for y_2/d_0 variation along the stream-wise direction was derived in the present study:

$$\frac{y_2}{d_0}=1-m\cdot\exp\left[0.21\cdot\frac{{Re_0}^{0.2}}{(\cos\alpha)^{0.5}}\right]\cdot\left(\frac{x}{d_0}\right)^{0.5}\cdot{Re_0}^{0.1} \quad (6)$$

This empirical relationship consists of three terms: (1) the approach flow turbulence conditions represented by Re_0, (2) the chute slope effect defined by the reference coordinate system relative to the buyout vector; and (3) the relative stream-wise direction x/d_0. In Eq. (6), m is a coefficient that may be related to the interaction with the upstream turbulent boundary layers and is affected by the wall roughness and pressure gate operation. For the present test data, $m = 0.80 \times 10^{-3}$. For the data of Killen (1968), $m = 1.20 \times 10^{-3}$. For the data of Chanson (1995), $m = 1.10 \times 10^{-3}$. For the prototype data of Cain (1978), $m = 0.24 \times 10^{-3}$.

Figs. 19 and 20 compare Eq. (6) and the measured data. The results showed satisfactory agreement for various initial Reynolds numbers and chute slopes and were further validated with the data of the previous models (Electronic Annex 1) and prototype. The parameter ranges of the present study's and literature's models included $4° \le \alpha \le 45°$, $1.0 \times 10^5 \le Re_0 \le 2.3 \times 10^6$, and $0 \le x/d_0 \le 300$. Therefore, Eq. (6) has a wide range of applicability for predicting the bottom self-aeration process.

Conclusions

The bottom self-aeration process is of interest to the mixture air–water aspects of the open channel flow. The air concentration profiles were measured, and the effects of the initial flow velocity, depth, and chute slope on the bottom self-aeration process were investigated by using a hydraulic model to systematically derive a data set. The following conclusions were developed

- With the increase of initial water flow velocity and depth, bottom self-aeration profiles locates closer to the chute bottom, and the diffusion of air bubbles into the self-aerated open channel flow becomes more pronounced. Because of such positive correlations, flow Reynolds number should be considered as an appropriate hydraulic condition for describing self-aeration development in open channel flows.
- With the increase of chute slope, the constraining effect of buoyancy on air bubble diffusion into the chute bottom gets decreased, which contributes to the development of the bottom self-aeration process affected by flow turbulence. For a flat chute, with the increase of flow turbulence level, the difference caused by slope variation is gradually more pronounced.
- A new equation to predict the bottom self-aeration process in chute flows is provided. The present result can be applied to $4° \le \alpha \le 45°$, $1.0 \times 10^5 \le Re_0 \le 2.3 \times 10^6$, and $0 \le x/d_0 \le 300$. Hence, further research is needed in order to study the influence of scale effect on self-aeration development in high-speed chute flows.

Acknowledgments

This work was funded by the National Natural Science Foundation of China (Nos. 51179113, 51379138) and Sichuan Province Funds for Distinguished Young Scientists (2013JQ0007).

Supplementary materials

Supplementary material associated with this article can be found, in the online version, at doi:10.1016/j.ijmultiphaseflow.2015.11.003.

References

Anwar, H.O., 1994. Self-aerated flows on chutes and spillways-discussion. J. Hydraul. Eng., ASCE 120 (6), 778–779.
Arreguin, F., Echavez, G., 1986. Natural Air entrainment in high velocity flows. In: Proceedings of Conference on advancements in Aerodynamics, Fluid Mech. and Hydraul., ASCE. Minneapolis, USA, pp. 186–192.
Cain, P., 1978. Measurements within Self-Aerated Flow on a Large Spillway Ph.D. thesis. University of Canterbury, New Zealand.
Chanson, H., 1993. Self-aerated flows on chutes and spillways. J. Hydraul. Eng., ASCE 119 (2), 220–243.
Chanson, H., 1995. Air bubble entrainment in free-surface turbulent flows. Department of civil engineering, The University of Queensland, Brisbane, Australia Experimental investigations Report No. CH46/95.
Chanson, H., 1997. Air bubble entrainment in open channels: Flow structure and bubble size distributions. Int. J. Multiphase Flow 23 (1), 193–203.
Chanson, H., 1997. Measuring air-water interface area in supercritical open channel flow. Water Res 31 (6), 1414–1420.
Chanson, H., 2013. Hydraulics of aerated flows: qui pro quo? J. Hydraul. Res., IAHR 51 (3), 223–243.
Chen, X.P., Shao, D.C., 2006. Measuring bubbles sizes in self-aerated flow. Water Resources Hydropower Eng 37 (10), 33–36 (in Chinese).
Deng, J., Xu, W.L., Qu, J.X., et al., 2002. Measurement and calculation of air concentration distribution of self-aerated flow in spillway tunnel. J. Hydraul. Eng. 4 (1), 64–68 (in Chinese).
Deng, J., Xu, W.L., Qu, J.X., et al., 2003. The influence of aeration on average velocity of self-aerated chute flow. J. Hydroelectric Eng. 83 (1), 88–94 (in Chinese).
Felder, S., Chanson, H., 2014. Triple decomposition technique in air–water flows: application to instationary flows on a stepped spillway. Int. J. Multiphase Flow 58, 139–153.
Guenther, P., Felder, S., Chanson, H., 2013. Flow aeration, cavitation processes and energy dissipation of flat and pooled stepped spillways for embankments. Environ. Fluid Mech. 13 (5), 503–525.
Hager, W.H., 1991. Uniform aerated chute flow. J. Hydraul. Eng., ASCE 118 (6), 528–533.
Hsiao, F., Lamb, O.P., Pilch, M., 1947. Report on the high velocity flow of water in a small rectangular channel. the University of Minnesota, Minneapolis, USA Project Report, Advanced Hydraulic Laboratory Nos. CE 194 and CE 195.
Hu, J.H., Zhou, W.J., Chen, Y.S., 2012. Ningbo is barricading against the challenge of Typhoon "Haikui" with emergency response. http://news.cnnb.com.cn/system/2012/08/07/007410404.shtml. (authorized by cnnb.com.cn) Accessed 7 August 2012. (in Chinese)
Isachenko, N.B., 1965. Effect of relative roughness of spillway surface on degrees of free-surface flow aeration. Izv. VNIIG 78, 350–357.
Killen, J.M., 1968. The surface characteristics of self-aerated flow in steep channels Ph.D. thesis. University of Minnesota, Minneapolis, USA.
Kramer, K., Hager, W.H., 2005. Air transport in chute flows. Int. J. Multiphase Flow 31 (10), 1181–1197.
Pagliara, S., Carnacina, I., Roshni, T., 2011. Inception point and air entrainment on flows under macroroughness condition. J. Environ. Eng., ASCE 137 (7), 629–638.
Pfister, M., Hager, W.H., 2010. Chute aerators. i: air transport characteristics. J. Hydraul. Eng., ASCE 136 (6), 352–359.
Pfister, M., Hager, W.H., 2010. Chute aerators. ii: hydraulic design. J. Hydraul. Eng., ASCE 136 (6), 360–367.
Pfister, M., Hager, W.H., 2011. Self-entrainment of air on stepped spillways. Int. J. Multiphase Flow 37 (2), 99–107.
Russell, S.O., Sheehan, G.J., 1974. Effect of entrained air on cavitation damage. Can. J. of Civ. Eng. 1 (1), 97–107.
Rasmussen, R.E.H., 1956. Some experiments on cavitation erosion in water mixed with air. In: Proceedings of NPL Symposium on Cavitation in Hydrodynamics. London, UK, pp. 1–25.
Straub, L.G., Anderson, A.G., 1958. Experiments on self-aerated flow in open channels. J. Hydraul. Div., ASCE 84 (7), 1–35.
Straub, L.G., Lamb, O.P., 1956. Studies of air entrainment in open-channel flows. Trans. ASCE 121, 30–44.
Wang, S.K., Lee, S.J., Jones, O.C., et al., 1990. Statistical analysis of turbulent two-phase pipe flow. J. Fluids Engrg., ASME 112, 89–95.

Wilhelms, S.C., 1997. Self-aerated spillway flow. University of Minnesota, USA Ph.D. thesis.
Wilhelms, S.C., Gulliver, J.S., 2005. Bubbles and waves description of self-aerated spillway flow. J. Hydraul. Res. 43 (6), 522–531.
Wood, I.R., 1983. Uniform region of self-aerated flow. J. Hydraul. Eng., ASCE 109 (3), 447–461.
Wood, I.R., 1991. Air entrainment in free-surface flows. IAHR hydraulic structures design manual no. 4. Hydraulic Design Considerations, Balkema Publ., Rotterdam, The Netherlands, p. 149.
Xi, R.Z., 1988. Characteristics of self-aerated flow on steep chutes. Proceedings of International Symposium on Hydraulics for High Dams. IAHR, Beijing, China, pp. 68–75.